

## Surface Modification by Compositionally Modulated Multilayered Zn-Fe Alloy Coatings

THANGARAJ, V.<sup>a</sup> RAVISHANKAR, K.<sup>b</sup> CHITHARANJAN HEGDE, A.\*<sup>a</sup>

<sup>a</sup> Department of Chemistry, National Institute of Technology Karnataka, Srinivasnagar 575025, India

<sup>b</sup> Department of Metallurgy and Materials Engineering, National Institute of Technology Karnataka, Srinivasnagar 575025, India

Compositionally modulated multilayered alloy (CMMA) coatings of Zn-Fe were developed from acid chloride baths by single bath technique. The production and properties of CMMA Zn-Fe coatings were tailored as a function of switching cathode current densities (SCCD's) and thickness of individual layers. Corrosion rates (CR) were measured by electrochemical methods. Corrosion resistances were found to vary with SCCD's and the number of sub layers in the deposit. SCCD's were optimized for production of Zn-Fe CMMA electroplates showing peak performance against corrosion. The formation of discrete Zn-Fe alloy layers having different compositions in the deposits were demonstrated by scanning electron microscopy (SEM). Improvements in the corrosion resistance of multilayered alloys are due to the inherent barrier properties of CMMA coatings as evidenced by electrochemical impedance spectroscopy (EIS). Corrosion resistance afforded by Zn-Fe CMMA coatings are explained in terms of the n-type semiconductor films at the interface, supported by Mott-Schottky's plot. It was observed that the alloy with high  $w(\text{Fe})$  on the top showed better corrosion resistance compared to that with the less  $w(\text{Fe})$  on top. At optimum SCCD's of 3.0—5.5  $\text{A}\cdot\text{dm}^{-2}$ , a Zn-Fe CMMA coatings with 600 sub layers showed *ca.* 45 times better corrosion resistance than conventional Zn-Fe alloy of the same thickness. The deposit showed no red rust even up to 1130 h in salt spray test.

**Keywords** electrodeposition, compositionally modulated multilayer alloy Zn-Fe coating, corrosion resistance

### Introduction

Recently electrolytic method of producing compositionally modulated multilayered coatings of Zn-M (where M is Fe group metals like Ni, Co and Fe) alloys received more attention in surface engineering because of their good corrosion resistance.<sup>1-9</sup> Compositionally modulated multilayered alloys (CMMA) coatings of Zn-based alloy can be achieved by means of two main techniques, known as the dual bath technique (DBT)<sup>10</sup> and the single bath technique (SBT).<sup>11</sup> In DBT, any combination of films can be formed, provided each can be individually deposited and very thin metal or alloy films can easily be formed. However, DBT has some disadvantages; the deposition process must be continually interrupted as the sample is transferred between baths and the danger exists of cross contamination due to drag out from each bath. As a result, the process is probably more time consuming. The drawbacks of DBT have been deemed to outweigh the benefits. In SBT, metal ions required to form both deposit layers, are included in a single electrolyte. To avoid simultaneous deposition of two metals, a large difference must exist between the deposition potentials of the two metals/alloys and this can be arranged by adjusting their deposition cathode current densities.

One of the earliest references to multilayer coatings was reported by Brenner and Pommer<sup>12</sup> who produced a multilayer Cu-Bi alloy from a single electrolyte. Cohen *et al.*<sup>13</sup> reported the production of Ag-Pd structures from a concentrated chloride bath, individual layer thicknesses were produced to values below 50 nm and the coating properties were seen to include reduced electrical resistivity and increased tarnish resistance. A large number of investigators have examined the Cu-Ni multilayer system. Barral and Maxmovitch<sup>14</sup> were one of the first investigators to examine this particular system. They operated a dual bath configuration depositing successive layers of zinc and nickel with individual layer thicknesses of 20—500 nm using a rotating disc electrode. Kalantary *et al.*<sup>15</sup> obtained Zn-Ni CMMA coatings with an overall thickness of 8  $\mu\text{m}$  by electrodepositing alternate layers of zinc and nickel from the zinc sulphate and nickel sulphate electrolytes. Chawa *et al.*<sup>3</sup> reported the corrosion resistance of Zn-Ni CMMA coatings from zinc sulphate and nickel sulphamate baths and showed that CMMA coatings have better corrosion resistance compared to that of monolithic coatings of zinc or nickel of a similar thickness. Recently, Liao *et al.*<sup>16-18</sup> have studied both single bath and dual bath of zinc/Zn-Fe and only Zn-Fe systems. Jensen *et al.*<sup>19</sup> have

\* E-mail: achegde@rediffmail.com; Fax: 0091-824-2474033

Received April 30, 2008; revised June 26, 2008; accepted August 6, 2008.

studied Zn-Fe CMMA coatings using SBT and DBT. Electrochemical stripping technique has been employed for analyzing the product and deposition process. Kirilova *et al.*<sup>20,21</sup> reported CMMA coatings of Zn-Co from SBT. They observed two separate peaks during the potentiodynamic stripping of a two layer coatings, corresponding to the dissolution of both metals independently of one another. Kirilova *et al.*<sup>22</sup> also studied the corrosion behavior of Zn-Co CMMA by corrosion potential measurement and salt spray tests. They reported that no red rust formation occurred on the surface even after 1584 h of salt spray corrosion testing on chromated CMMA Zn-Co coatings.

Thus enormous amount of literature is available on multilayered deposition of Zn-Ni (and even Zn-Co) alloy coatings for improved corrosion resistance using double bath. Because of the limitation of anomalous codeposition, a characteristic feature of Zn-Fe group metal alloys, under normal working conditions the deposition of individual metals are highly impossible using single bath technique.<sup>12</sup> Hence no work is reported with regard to the production of CMMA coatings of Zn-Fe group metal alloys over steel for improved protection against corrosion. In this regard, the present paper reports the method of optimizing the deposition conditions for production of CMMA Zn-Fe coatings showing peak performance against corrosion. Corrosion data of CMMA Zn-Fe alloy coatings are compared with that of bulk metal and monolithic coatings of constituting metals. Factors responsible for significant improvement in corrosion resistance were analyzed and discussed.

## Experimental

Hull cell study revealed that in monolithic Zn-Fe alloy, the  $w(\text{Fe})$  in the alloy increase gradually with current density employed for deposition. The fact that a small change in  $w(\text{Fe})$  brings a large change in the phase structure and hence the properties of Zn-Fe deposits have been exploited in the present work. On the other hand, because of the complexity of anomalous codeposition in Zn-Fe group metal alloys, it is all most impossible to deposit of either pure Zn or pure Fe in layered manner using single bath technique. Hence, the only possibility to bring modulation in compositions of alloys is by bringing modulation in cathode current densities at which their codepositions are taking place. Therefore, two layers of alloys having different compositions were deposited one over another by depositing the alloy at two different cathode current densities. Deposition time may be varied depending on the thickness of each alloy layer required. The process was made to repeat for required number of times depending on the thicknesses of deposits required.

Computerized power source was used to produce CMMA Zn-Fe coatings with great degree of accuracy and reproducibility. The power source was set to switch between the two cathode current densities called

switching cathode current densities (SCCD's) to get an array of alloys of having different compositions. At low current density, Zn-Fe alloy of one composition, represented by  $(\text{Zn-Fe})_1$  and at high current density Zn-Fe alloy of another composition, represented by  $(\text{Zn-Fe})_2$  were deposited. CMMA coatings represented by  $(\text{Zn-Fe})_1/(\text{Zn-Fe})_2$  [layer with less  $w(\text{Fe})$  on steel substrate and layer with more  $w(\text{Fe})$  on top] were developed at two cathode current densities. CMMA coatings developed by reversing the sequence of SCCD's are represented as  $(\text{Zn-Fe})_2/(\text{Zn-Fe})_1$  [layer with more  $w(\text{Fe})$  on steel substrate and layer with less  $w(\text{Fe})$  on top]. Vertical line between alloys of different compositions represents phase boundary between sublayers.

In the present study, CMMA Zn-Fe coatings were produced from single bath containing 110 g (0.8 mol)  $\text{ZnCl}_2$ , 40 g (0.2 mol)  $\text{FeCl}_3$ , 180 g (3.4 mol)  $\text{NH}_4\text{Cl}$  and 60 g (0.8 mol)  $\text{KCl}$  in the presence of 8 g glycine and 2 g of citric acid. All depositions were carried out galvanostatically in an electrolytic cell of 500 mL capacity made up of Perspex material with keeping cathode at 4 cm distance from anode. Pre-cleaned mild steel panels were used as cathode and pure zinc as anode. Coatings were carried out in a constantly stirred electrolyte maintained at 30 °C. All coatings were carried out for duration of 10 min for the purpose of comparison. CMMA coatings and subsequent characterization was done using Electrochemical Workstation (Metrohm PGSTAT 30).

SEM (JEOL 6380 LA, Japan) was used for examining the cross sectional and surface morphology of CMMA deposits. Compositions of deposits were determined by colorimetric method at 480 nm by stripping the deposit in dilute HCl using inhibitor. Corrosion resistances of coatings were evaluated by electrochemical methods using saturated calomel electrode (SCE) as reference and platinum electrode as counter. Corrosion study were made in a stagnant aerated 5% NaCl solution, pH 6, at 25 °C at a scan rate 1.0 mV/s in the potential ramp of 0.5 V cathodic and 1.5 V anodic from open circuit potential (OCP). Corrosion rates were determined by Tafel's extrapolation method through the values of corrosion current ( $i_{\text{corr}}$ ) and corrosion current density ( $I_{\text{corr}}$ ). Electrochemical impedance spectroscopy (EIS) technique was used to evaluate the corrosion resistance of deposits in terms film capacitance in the frequency range of 100 kHz to 20 mHz. Factors responsible for improved corrosion resistance were explained through improved electronic properties of the film, supported by M-S plot. Importance of ending layer in CMMA coatings was tested in terms of its corrosion resistance. Corrosion rates of CMMA coatings were studied by neutral salt spray tests, as per ASTM B117.

## Results and discussion

### Zn-Fe alloy coating

Smooth and uniform monolithic Zn-Fe alloy coat-

ings were carried out on mild steel at current density of 3.0 and 5.0 A/dm<sup>2</sup> from the optimized bath. The deposit having *ca.* 0.8–1.4 w(Fe) was found to show corrosion rate (CR) of  $72.5 \times 10^{-2}$  and  $81.5 \times 10^{-2}$  mm/y, respectively, as shown in Table 1. The corrosion resistance of Zn-Fe alloys were tried to increase further by nanostructured multilayered coatings of Zn and Fe.

### CMMA Zn-Fe coatings

**Optimization of switching cathode current densities (SCCD's)** CMMA coatings were developed on pre-cleaned mild steel panels using optimized Zn-Fe alloy plating bath. To bring large modulation in compositions of alloys, depositions were carried out at different SCCD's varying difference. Electroplates represented by (Zn-Fe)<sub>1</sub>/(Zn-Fe)<sub>2</sub> (where 1 and 2 correspond low and high current densities, respectively) were produced with difference of 1.0, 1.5 and 2.5 A/dm<sup>2</sup> between SCCD's for possible improvements in corrosion resistance. To begin with, CMMA coatings were carried out to get 20 sub layers of alloys with 30 s deposition time each (for total 10 min). Corrosion rates of coatings under different SCCD's were evaluated and data are reported in the Table 1. It was found that among different set of SCCD's, only at 3.0–4.5 and 3.0–5.5 A/dm<sup>2</sup>, the CMMA coatings showed less corrosion rate ( $26.94 \times 10^{-2}$  and  $8.54 \times 10^{-2}$  mm/y, respectively) as shown in Table 1. Almost constant corrosion rates were observed at other set of SCCD's, may be due to diffused sublayers without any phase change. Therefore, 3.0–

4.5 and 3.0–5.5 A/dm<sup>2</sup> have been taken for further layering to achieve more corrosion protection.

**Optimization of thickness of sub layers** The fact that a small compositional change of alloys brings a significant change in phase structure of the deposit and the metallurgical properties of CMMA coatings can be improved further by increasing the numbers of sublayers without sacrificing the demarcation between sublayers have been used extensively for improving the corrosion resistance of CMMA deposits. By keeping current density 3.0–4.5 and 3.0–5.5 A/dm<sup>2</sup> as SCCD's, deposition was carried out with 30, 60, 120, 300 and 600 sublayers. The CR of coatings was found to decrease with number of sub layers as shown in Table 2. At 3.0–4.5 A/dm<sup>2</sup>, coatings having 600 sublayers showed minimum CR of  $16.44 \times 10^{-2}$  mm/y against  $72.15 \times 10^{-2}$  mm/y for conventional Zn-Fe alloy coatings. But, a substantial decrease of CR ( $1.65 \times 10^{-2}$  mm/y) was exhibited by coatings having 600 sub layers at 3.0–5.5 A/dm<sup>2</sup> as shown in Table 2. Corrosion rates of CMMA coatings represented by (Zn-Fe)<sub>1</sub>/(Zn-Fe)<sub>2</sub> were found to decrease on reversing the sequence of SCCD's as shown in Table 3. *i.e.* by reversing the sequence cathode current density, an alloy with high w(Fe) (1.2%) on top changed to low w(Fe) (0.90%). Corrosion data reported in Tables 2 and 3 show that CMMA coatings with (Zn-Fe)<sub>2</sub>/(Zn-Fe)<sub>1</sub> configurations is more susceptible for corrosion than coatings with (Zn-Fe)<sub>1</sub>/(Zn-Fe)<sub>2</sub> configuration in all degrees of layering.

**Table 1** Corrosion rate (CR) of CMMA Zn-Fe coatings at different conditions from optimized bath

SCCD's/(A•dm <sup>-2</sup> )	$-E_{\text{corr}}/V$ (vs. SCE)	$I_{\text{corr}}/(\mu\text{A}\cdot\text{cm}^{-2})$	CR/(10 <sup>-2</sup> mm•y <sup>-1</sup> )
CMMA (Zn-Fe) <sub>1</sub> /(Zn-Fe) <sub>2</sub> alloy coating with 1.0 A/dm <sup>2</sup> difference (20 sublayers)			
1.0–2.0	1.158	54.84	80.13
2.0–3.0	1.114	52.82	77.18
3.0–4.0	1.262	37.26	54.40
4.0–5.0	1.245	36.09	54.23
CMMA (Zn-Fe) <sub>1</sub> /(Zn-Fe) <sub>2</sub> alloy coating with 1.5 A/dm <sup>2</sup> difference (20 sublayers)			
1.0–2.5	1.049	33.85	50.87
2.0–3.5	1.011	26.69	40.11
3.0–4.5	1.362	17.92	26.94
4.0–5.5	1.282	22.75	34.19
CMMA (Zn-Fe) <sub>1</sub> /(Zn-Fe) <sub>2</sub> alloy coating with 2.5 A•dm <sup>-2</sup> difference (20 sublayers)			
3.0–5.5	1.119	5.684	8.54
Monolithic Zn-Fe coating			
Current density/(A•dm <sup>-2</sup> )	$-E_{\text{corr}}/V$ (vs. SCE)	$I_{\text{corr}}/(\mu\text{A}\cdot\text{cm}^{-2})$	CR/(10 <sup>-2</sup> mm•y <sup>-1</sup> )
3.0	1.080	49.41	72.5
5.0	1.116	55.84	81.5

**Table 2** Decrease of corrosion rate (CR) of CMMA coatings with increase of sublayers

Current density/(A·dm <sup>-2</sup> )	Number of sublayers	-E <sub>corr</sub> /V (vs. SCE)	I <sub>corr</sub> /(μA·cm <sup>-2</sup> )	CR/(10 <sup>-2</sup> mm·y <sup>-1</sup> )
Optimization of sublayer thickness at SCCD's of 3.0—4.5 A·dm <sup>-2</sup>				
3.0—4.5	20	1.362	17.92	26.94
3.0—4.5	30	1.275	15.93	23.93
3.0—4.5	60	1.294	15.17	22.80
3.0—4.5	120	1.120	12.79	19.22
3.0—4.5	300	1.087	10.94	16.86
3.0—4.5	600	1.091	11.22	16.44
Optimization of sublayer thickness at SCCD's 3.0—5.5 A·dm <sup>-2</sup>				
3.0—5.5	20	1.119	5.684	8.54
3.0—5.5	30	1.103	3.789	5.69
3.0—5.5	60	1.293	3.308	4.97
3.0—5.5	120	1.162	2.616	3.93
3.0—5.5	300	1.089	1.675	2.52
3.0—5.5	600	1.143	1.117	1.65

**Table 3** Effect of reversing the sequence of SCCD's and degree of layering on corrosion rate

Current density/(A·dm <sup>-2</sup> )	Number of sublayers	-E <sub>corr</sub> /V (vs. SCE)	I <sub>corr</sub> /(μA·cm <sup>-2</sup> )	CR/(10 <sup>-2</sup> mm·y <sup>-1</sup> )
Effect of reversing the sequence of layering at 4.5—3.0 A·dm <sup>-2</sup>				
4.5—3.0	20	1.191	15.57	23.40
4.5—3.0	30	1.102	14.07	21.14
4.5—3.0	60	1.258	13.69	20.58
4.5—3.0	120	1.269	13.32	20.01
4.5—3.0	300	1.210	12.43	18.67
4.5—3.0	600	1.313	11.77	17.68
Effect of reversing the sequence of layering at 5.5—3.0 A·dm <sup>-2</sup>				
5.5—3.0	20	1.257	8.261	12.21
5.5—3.0	30	1.107	7.228	10.73
5.5—3.0	60	1.100	6.524	9.68
5.5—3.0	120	1.208	4.869	7.23
5.5—3.0	300	1.212	3.171	4.71
5.5—3.0	600	1.071	1.679	2.49

### Corrosion study

**Tafel's polarization study** Tafel's polarization curve of CMMA electroplates having different numbers of sublayers are shown in Figure 1. The first peak in anodic polarization curve corresponds to the dissolution of zinc in coatings. The increases of sublayers have increased the barrier properties of the coatings, which are evident from the low  $i_{\text{corr}}$  values reported. Further, the progressive decrease of anodic current with number of sub layers indicate that improved corrosion resistance are due to barrier protection of coatings. CMMA coatings with 600 sub layers showed the lowest CR. Hence, CMMA coating with (Zn-Fe)<sub>1</sub>/(Zn-Fe)<sub>2</sub> configuration is properly modulated by its composition. Thus CMMA Zn-Fe coatings (at 3.0—5.5 A·dm<sup>-2</sup> with 600 sublayers

having (Zn-Fe)<sub>1</sub>/(Zn-Fe)<sub>2</sub> configuration) were found to be ca. 45 times more corrosion resistant compared to monolithic Zn-Fe coatings of same thickness (Table 3).

**Electrochemical impedance spectroscopy (EIS)** Nyquist responses of CMMA Zn-Fe coatings at optimized SCCD's with different number of sublayers are shown in Figure 2. EIS is a suitable technique to gain valuable information on the capacitance behavior of double layer, responsible for improved corrosion resistance of CMMA coatings. Semicircles in Figure 2 clearly indicates that the capacitance of the double layer has increased drastically with increase of number of sublayers and improved corrosion resistance afforded by CMMA coatings are due to the improved semiconductor behavior of deposits.

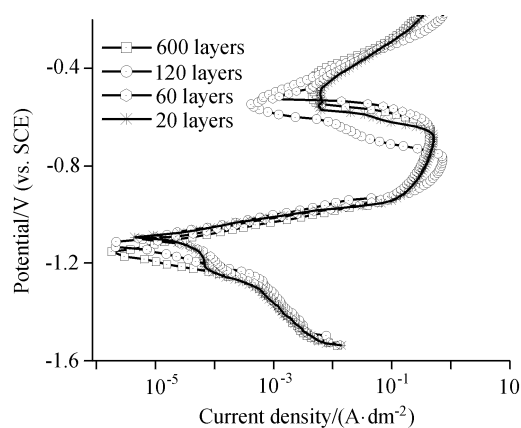


**Figure 1** Potentiodynamic polarization curves of CMMA  $(\text{Zn-Fe})_1/(\text{Zn-Fe})_2$  coatings with different number of sublayers (1.0 mV/s).

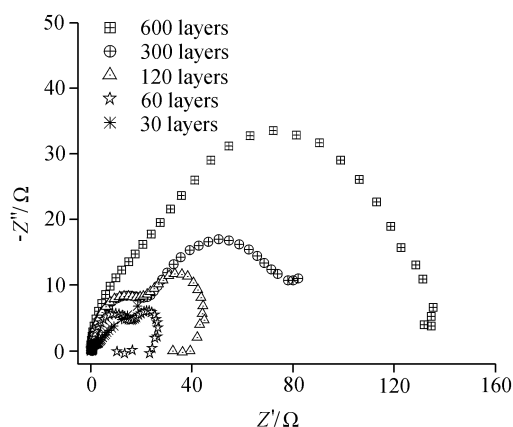


**Figure 2** Nyquist plots of CMMA  $(\text{Zn-Fe})_1/(\text{Zn-Fe})_2$  coatings having different number of sublayers.

**Mott-Schottky plot for CMMA coatings** Substantial decrease of CR with CMMA coatings are attributed to the structural and electronic properties of passive film at the interface as evidenced by Mott-Schottky plot in Figure 3. Improved corrosion resistances are attributed to the formation of semiconductor film at the

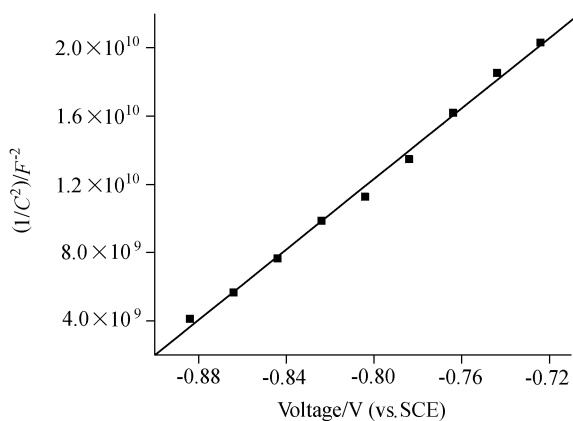


**Figure 3** Mott-Schottky plots for CMMA  $(\text{Zn-Fe})_1/(\text{Zn-Fe})_2$  coating.

interface. Further, the positive slope of the graph reveal that n-type semiconductor film is operative in controlling corrosion of nanostructured coatings. The deposits with large number of sublayers (with smaller thicknesses) are believed to impart more semiconductor behavior to the deposit.

**SEM image of CMMA coatings** Samples of CMMA Zn-Fe coatings were assessed initially by their surface appearance. All the specimens show a satisfactory appearance and almost no surface drawback was found by naked eye. The cross-sectional view of Zn-Fe CMMA coatings with 20 sublayers observed under SEM is shown in Figure 4a. Unlike CMMA Zn-Ni and CMMA Zn-Co, SEM images of CMMA Zn-Fe coatings have not shown good contrast between the sublayers. Inherent micro cracks developed during ultra-layering may be responsible for cross layered structure as in Figures 4a and 4b. The difference in the surface morphology of CMMA  $(\text{Zn-Fe})_1/(\text{Zn-Fe})_2$  coatings (with 20 sublayers) and monolithic Zn-Fe alloy coatings are shown in Figures 4c and 4d. Pores and perhaps micro cracks visible on CMMA coatings may be due to the stronger tensile stress developed on high  $w(\text{Fe})$  top layer. However, they do not decrease its protective performance due to many underlying sublayers.

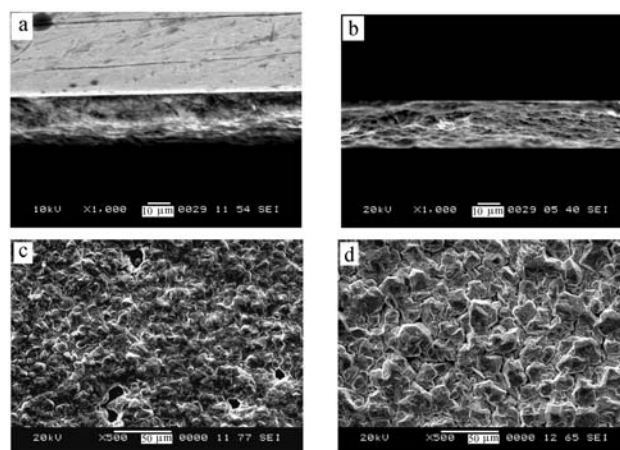


**Figure 4** Photomicrograph of CMMA  $(\text{Zn-Fe})_1/(\text{Zn-Fe})_2$  coatings cross sectional view at (a) 10 and (b) 20 kV, (c) surface morphology of CMMA Zn-Fe (20 sublayers) and (d) surface morphology of monolithic Zn-Fe alloy.

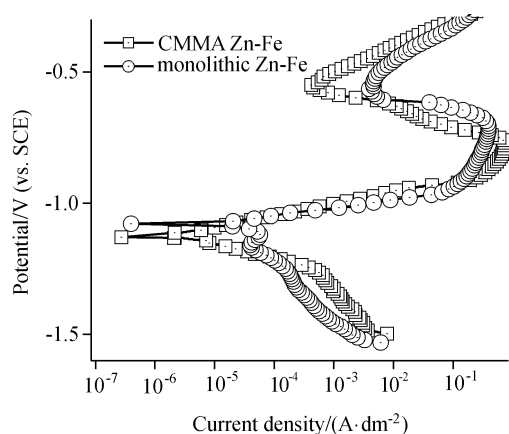
### Comparison of corrosion performance of monolithic Zn-Fe alloy and CMMA Zn-Fe alloy

Corrosion rates of monolithic alloy of Zn-Fe alloy and CMMA  $(\text{Zn-Fe})_1/(\text{Zn-Fe})_2$  and CMMA  $(\text{Zn-Fe})_2/(\text{Zn-Fe})_1$  coatings are given in Table 4. It was found that CMMA Zn-Fe coatings are more corrosion resistant ( $1.65 \times 10^{-2}$  mm/y) compared to homogenous alloy of same thickness. The coatings with  $(\text{Zn-Fe})_1/(\text{Zn-Fe})_2$  configuration was found to have alloy high  $w(\text{Fe})$  (1.25%) on top. Further, on reversing the SCCD's, the corrosion rate was found to be  $2.49 \times 10^{-2}$  mm/y. The less corrosion tendency with reverse  $(\text{Zn-Fe})_2/(\text{Zn-Fe})_1$  configuration is due to less  $w(\text{Fe})$  (0.90%) alloy on

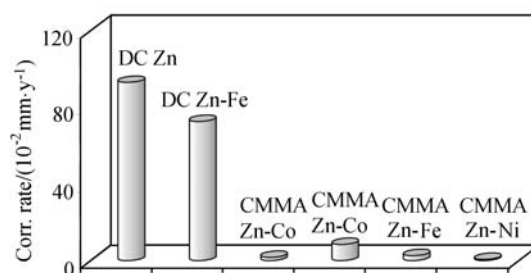
**Table 4** Comparison of corrosion rates (CR) of CMMA Zn-Fe coatings at different configurations and monolithic Zn-Fe alloy of same thickness

Coating system	Number of sublayers	Cathode current density/ ( $\text{A}\cdot\text{dm}^{-2}$ )	$-E_{\text{corr}}/\text{V}$ (vs SCE)	$I_{\text{corr}}/(\mu\text{A}\cdot\text{cm}^{-2})$	CR/( $10^{-2}\text{ mm}\cdot\text{y}^{-1}$ )
Monolithic Zn-Fe alloy	Monolithic alloy	3.0	1.080	49.417	72.15
	Without layering	5.0	1.116	55.849	81.54
CMMA	600	3.0—4.5	1.091	11.22	16.86
(Zn-Fe) <sub>1</sub> /(Zn-Fe) <sub>2</sub>	600	3.0—5.5	1.143	1.117	1.65
CMMA	600	4.5—3.0	1.313	11.77	17.68
(Zn-Fe) <sub>2</sub> /(Zn-Fe) <sub>1</sub>	600	5.5—3.0	1.071	1.679	2.49

the top. Hence the corrosion protection ability of CMMA Zn-Fe coatings depends on the ending current density during deposition. The polarizations curves of CMMA Zn-Fe coatings with (Zn-Fe)<sub>1</sub>/(Zn-Fe)<sub>2</sub> and monolithic Zn-Fe alloy coatings are shown in Figure 5. Less corrosion rate observed in (Zn-Fe)<sub>1</sub>/(Zn-Fe)<sub>2</sub> configuration compared to that in (Zn-Fe)<sub>2</sub>/(Zn-Fe)<sub>1</sub> configuration is attributed to high  $w(\text{Fe})$  alloy on the top. As a whole, it may be thought that the protection efficacy of CMMA Zn-Fe coatings depends on the barrier effect of (Zn-Fe)<sub>2</sub> alloy sublayers and sacrificial effect of (Zn-Fe)<sub>1</sub> sublayers.

**Figure 5** Comparison of potentiodynamic polarization behavior of CMMA Zn-Fe deposits and monolithic Zn-Fe alloys of same thickness at scan rate  $1.0\text{ mV}\cdot\text{s}^{-1}$ .

Corrosion performance of CMMA coated samples was also examined by neutral salt spray corrosion test. All the CMMA Zn-Fe coatings gave a longer time to red rust than monolithic Zn-Fe coatings with same thickness. CMMA Zn-Fe coatings showed red rust after 1034 h against to 528 h for monolithic Zn-Fe alloy. A comparison of corrosion rates of Zn, Zn-Fe, CMMA (Zn-Fe)<sub>1</sub>/(Zn-Fe)<sub>2</sub>, CMMA (Zn-Fe)<sub>2</sub>/(Zn-Fe)<sub>1</sub>, CMMA (Zn-Co)<sub>1</sub>/(Zn-Co)<sub>2</sub>, CMMA (Zn-Ni)<sub>1</sub>/(Zn-Ni)<sub>2</sub> coatings of same thickness is shown in Figure 6. It was found that corrosion rate of CMMA (Zn-Fe)<sub>1</sub>/(Zn-Fe)<sub>2</sub> coatings ( $1.65 \times 10^{-2}\text{ mm/y}$ ) is less than that of CMMA (Zn-Fe)<sub>2</sub>/(Zn-Fe)<sub>1</sub> coating ( $2.49 \times 10^{-2}\text{ mm/y}$ ) of same thickness but much less than (about 43 times) mono-

**Figure 6** Comparison of corrosion rates of Zn, monolithic Zn-Fe, CMMA (Zn-Fe)<sub>1</sub>/(Zn-Fe)<sub>2</sub>, CMMA (Zn-Fe)<sub>2</sub>/(Zn-Fe)<sub>1</sub>, CMMA (Zn-Co)<sub>1</sub>/(Zn-Co)<sub>2</sub>, CMMA (Zn-Ni)<sub>1</sub>/(Zn-Ni)<sub>2</sub> coatings of same thickness.

lithic alloy of Zn-Fe.

## Conclusion

Corrosion resistance of Zn-Fe alloy coatings can be increased to several fold of its magnitude by compositionally modulated multilayered alloy (CMMA) coating by proper modulation of compositions of sublayers. Nano-structured multilayered coatings show considerable improvement in its corrosion performance compared to homogenous alloy of same metals having same thickness. The sequence of layering also plays an important role in controlling the rate of corrosion. The more the  $w(\text{Fe})$  in the alloy on the top, the better its corrosion resistance. Corrosion resistance afforded by CMMA is explained by the formation of a semi conductive surface film at the interface, supported by Mott-Schottky plot. Protection efficacy of CMMA Zn-Fe coatings depends on the barrier effect of alloy sublayer having high  $w(\text{Fe})$  and sacrificial effect of alloy sublayer having less  $w(\text{Fe})$ . CMMA Zn-Fe coating obtained at current density of  $3.0\text{--}5.5\text{ A/dm}^2$  with 600 alternate layers of each metal showed about *ca.* 45 times better corrosion resistance compared to that of conventional Zn-Fe alloy coatings. From comparison of corrosion rates of Zn, Zn-Fe, CMMA Zn-Co, CMMA Zn-Ni, CMMA Zn-Fe and CMMA Fe-Zn alloy coatings of same thickness, it may be concluded that corrosion rate of CMMA Zn-Fe coatings ( $1.65 \times 10^{-2}\text{ mm/y}$ ) is less than that of CMMA Zn-Ni coating ( $0.54 \times 10^{-2}\text{ mm/y}$ ) but higher than monolithic Zn-Co and Zn-Ni alloys of same thickness.

## References

- 1 Gabe, D. R.; Green, W. A. *Surf. Coat. Technol.* **1998**, *105*, 195.
- 2 Nabiyouni, G.; Schwarzacher, W.; Rolik, Z.; Bakonyi, I. *J. Magn. Magn Mater.* **2002**, *253*, 77.
- 3 Chawa, G.; Wilcox, G. D.; Gabe, D. R. *Trans. IMF* **1998**, *76*, 117.
- 4 Haseeb, A.; Celis, J. P.; Roos, J. R. *J. Electrochem. Soc.* **1994**, *141*, 230.
- 5 Swathirajan, S. *J. Electrochem. Soc.* **1986**, *133*, 671.
- 6 Despic, A. R.; Jovic, V. D. *J. Electrochem. Soc.* **1987**, *134*, 3004.
- 7 Despic, A. R.; Jovic, V. D. *J. Electrochem. Soc.* **1989**, *136*, 1651.
- 8 Wilcox, G. D.; Gabe, D. R. *Corros. Sci.* **1993**, *35*, 1251.
- 9 Kalantary, M. R. *Plat. Surf. Finish.* **1994**, *81*, 80.
- 10 Haseeb, A. S. M. A.; Celis, J. P.; Roos, J. R. *J. Electrochem. Soc.* **1994**, *141*, 230.
- 11 Lashmore, D. S.; Dariel, M. P. *J. Electrochem. Soc.* **1988**, *135*, 1218.
- 12 Brenner, A. *Electrodeposition of Alloys' Principles and Practice*, Vol. II, Academic Press, New York, **1963**, p. 589.
- 13 Cohen, U.; Koch, F. B.; Sard, R. *Electrochemical Society, Meeting*, Orlando, USA, **1981**.
- 14 Barral, G.; Maximovitch, S. *Colloque de Physique* **1990**, *51*, PC4-291.
- 15 Kalantary, M. R.; Wilcox, G. D.; Gabe, D. R. *British Corr. J.* **1998**, *33*, 197.
- 16 Liao, Y.; Gabe, D. R.; Wilcox, G. D. *Plat. Surf. Finish.* **1998**, *85*, 60.
- 17 Liao, Y.; Gabe, D. R.; Wilcox, G. D. *Plat. Surf. Finish.* **1998**, *85*, 62.
- 18 Liao, Y.; Gabe, D. R.; Wilcox, G. D. *Plat. Surf. Finish.* **1998**, *85*, 88.
- 19 Jensen, J. D.; Gabe, D. R.; Wilcox, G. D. *Surf. Coat. Technol.* **1998**, *105*, 240.
- 20 Kirilova, I.; Ivanov, I.; Rashkov, S. *J. Appl. Electrochem.* **1998**, *28*, 637.
- 21 Kirilova, I.; Ivanov, I.; Rashkov, S. *J. Appl. Electrochem.* **1998**, *28*, 1359.
- 22 Kirilova, I.; Ivanov, I. *J. Appl. Electrochem.* **1999**, *29*, 1133.

(E0804301 DING, W. F.)